Trends in R−X Bond Dissociation Energies (R = Me, Et, *i*-Pr, *t*-Bu; X = H, CH₃, OCH₃, OH, F): A Surprising Shortcoming of Density Functional Theory

Ekaterina I. Izgorodina,[†] Michelle L. Coote,*,[†] and Leo Radom*,[‡]

Research School of Chemistry, Australian National University, Canberra, ACT 0200, Australia, and School of Chemistry, University of Sydney, Sydney, NSW 2006, Australia
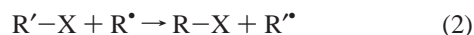
The performance of a variety of high-level composite procedures, as well as lower-cost density functional theory (DFT)- and second-order perturbation theory (MP2)-based methods, for the prediction of absolute and relative R−X bond dissociation energies (BDEs) was examined for R = Me, Et, *i*-Pr and *t*-Bu, and X = H, CH₃, OCH₃, OH and F. The methods considered include the high-level G3(MP2)-RAD and G3-RAD procedures, a variety of pure and hybrid DFT methods (B-LYP, B3-LYP, B3-P86, KMLYP, B1B95, MPW1PW91, MPW1B95, BB1K, MPW1K, MPWB1K and BMK), standard restricted (open-shell) MP2 (RMP2), and two recently introduced variants of MP2, namely spin-component-scaled MP2 (SCS-MP2) and scaled-opposite-spin MP2 (SOS-MP2). The high-level composite procedures show very good agreement with experiment and are used to evaluate the performance of the lower-level DFT- and MP2-based procedures. The best DFT methods (KMLYP and particularly BMK) provide very reasonable predictions for the absolute heats of formation and R−X BDEs for the systems studied. However, all of the DFT methods overestimate the stabilizing effect on BDEs in going from R = Me to R = *t*-Bu, leading in some cases to incorrect qualitative behavior. In contrast, the MP2-based methods generally show larger errors (than the best DFT methods) in the absolute heats of formation and BDEs, but better behavior for the relative BDEs, although they do tend to underestimate the stabilizing effect on BDEs in going from R = Me to R = *t*-Bu. The potentially less computationally expensive SOS-MP2 method offers particular promise as a reliable method that might be applicable to larger systems.

1. Introduction

The bond dissociation energy (BDE) is an important fundamental concept in chemistry. It is used as a measure of the strength of a chemical bond and is defined as the enthalpy change for the dissociation reaction:

$$R-X \rightarrow R^{\bullet} + {}^{\bullet}X \tag{1}$$

Relative values of BDEs are also extremely important in chemistry. For example, the difference between the R′−X and R−X BDEs is effectively the enthalpy change for the X-transfer reaction:

$$R'-X + R^{\bullet} \rightarrow R-X + R'^{\bullet} \tag{2}$$

Moreover, when X = H and R′ = CH₃, the enthalpy change for reaction 2 is defined as the radical stabilization energy (RSE) for the radical R• and is often used as a measure of radical stability. The accurate prediction of BDEs and RSEs has numerous applications, including the identification of sites for potential free-radical attack in peptides, the assessment of the effectiveness of antioxidants, and the study of chain-transfer processes (such as long-chain branching) in free-radical polymerization. However, for useful practical applications in large polymer-related or biologically related systems to be feasible,

it is necessary to identify reliable low-cost methods to calculate these quantities.

Density functional theory (DFT) is now widely used as a computational chemistry tool and is found to provide reasonable accuracy at modest computational cost for a wide range of chemical systems.[1] Although there are several types of calculation (notably reaction barrier heights[2,3] and heats of formation[4−6]) for which popular DFT methods such as B3-LYP are known to show substantial errors in some cases, the calculation of relative BDEs (such as RSEs and the enthalpies of abstraction reactions) is not normally regarded as problematic. For instance, Brinck et al.[7] concluded that, although the absolute BDEs were unreliable, the B3-LYP method was suitable for the prediction of the effect of substituents on the C−H BDEs in substituted methanes, C−O BDEs in peroxyl radicals, and O−H BDEs in hydroperoxides. We have also noted that B3-LYP underestimates C−H BDEs but, through a systematic cancellation of errors, generally produces reasonable values of RSEs.[8] In a number of recent assessment studies, Truhlar and co-workers have indicated that methods such as B3-LYP, though inadequate for the prediction of barrier heights, nonetheless perform well for the enthalpies of hydrogen-abstraction reactions and also for bond dissociation energies.[2] We have also shown that the B3-LYP method provides reasonable performance for the enthalpies of hydrogen-atom-abstraction reactions involving substituted carbon-centered radicals, and the associated C−H BDEs of the closed-shell reactants and RSEs of the open-shell reactants.[9] Finally, Chen and Bozzelli[10] have noted that the B3-LYP method models very well the relative heats of formation

* Corresponding authors. E-mail: (M.L.C.) mcoote@rsc.anu.edu.au; (L.R.) radom@chem.usyd.edu.au.
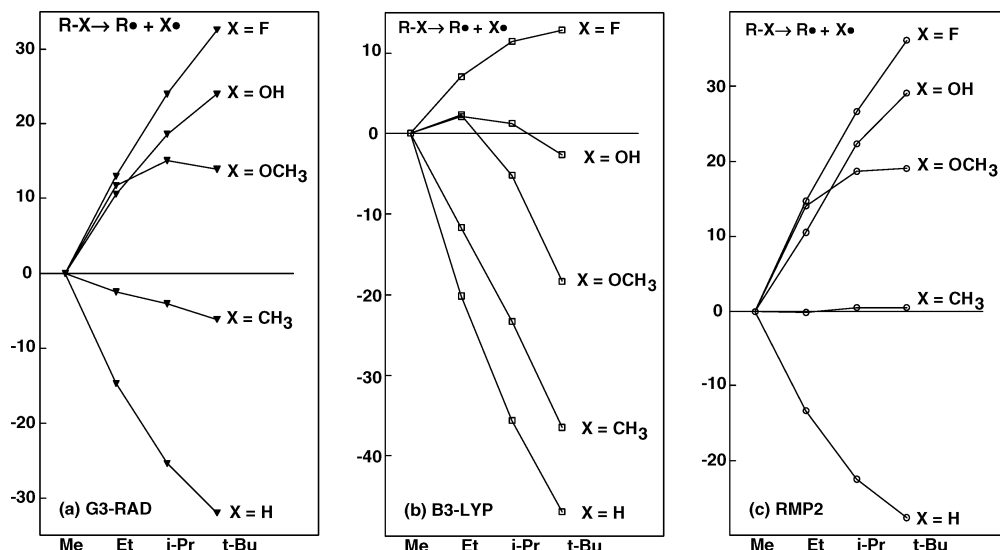† Australian National University.
‡ University of Sydney.

Trends in R−X Bond Dissociation Energies

J. Phys. Chem. A, Vol. 109, No. 33, 2005 **7559**

Figure 1. Trends in relative R−X bond dissociation energies (0 K, kJ mol^{-1}) for R = Me, Et, *i*-Pr, *t*-Bu and X = H, CH$_3$, OCH$_3$, OH, F, as calculated via (a) G3-RAD, (b) B3-LYP/6-311+G(3df,2p), and (c) RMP2/G3MP2large.

and BDEs of the R−OCH$_3$ ethers (R = Me, Et, *i*-Pr, *t*-Bu). However, it should be noted that in this study the heats of formation and BDEs were calculated via an isodesmic method that allowed for substantial cancellation of error.

In contrast to these previous studies, we recently discovered a significant problem in the prediction of the relative R−X BDEs (R = Me, Et, *i*-Pr, *t*-Bu; X = H, CH$_3$, OCH$_3$, OH, F) using B3-LYP.[11] The background to this discovery was our finding, based on calculations with high-level composite procedures such as G3-RAD, that these systems exhibit unusual trends in the BDEs with respect to increasing alkylation of R,[12] trends that are also shown by the available experimental data.[13,14] In essence, as R goes from Me to *t*-Bu, the product radical R$^{\bullet}$ is expected to become more stable, due to the influence of additional methyl groups interacting by hyperconjugation with the radical center, and this would contribute to a more favorable (lower) bond dissociation energy as we go from Me to *t*-Bu. However, this BDE-lowering influence of increasing alkylation is countered by the increasing stabilization of the R−X bond through increased resonance between its covalent (R−X) and ionic (R$^+$ X$^-$) forms.[12] As R becomes more substituted (from Me to *t*-Bu), its electron-donating ability increases, the relative stability of the ionic configuration (and thus the stabilization of the bond via resonance) increases, and hence the bond dissociation reaction is expected to become *less* favorable from Me to *t*-Bu. The relative importance of the BDE-lowering effect and the BDE-raising effect depends of course upon the electronegativity of X. Thus when X = H, the ionic configurations are not very significant and the BDE-lowering effect of increasing alkylation on the stability of R$^{\bullet}$ dominates. As a result, the BDEs in the R−H series decrease from Me to *t*-Bu in accordance with the increasing radical stability. In contrast, when X is the electronegative F substituent, the BDE-raising effect of increasing alkylation on the stability of R−X dominates, and the BDEs in the R−F series increase from Me to *t*-Bu. The other X-substituents have intermediate electronegativities and thus show intermediate (and at times nonmonotonic) trends (see Figure 1a).

However, we found in our study that the B3-LYP method failed in some cases even to reproduce the qualitative trends in these relative BDEs (see Figure 1b).[11] In general, the B3-LYP method significantly underestimates the stabilizing effect of increasing alkylation on both the R−X molecules and the R$^{\bullet}$

radicals, consistent with previous findings that B3-LYP systematically underestimates the stability of larger molecules.[15] Because the errors in the R−X molecules are substantially greater than those in R$^{\bullet}$, the net result is to overestimate the BDE-lowering effect of increasing alkylation on the R−X BDEs. This problem is particularly evident in the R−O BDEs (i.e., the R−OH and R−OCH$_3$ series). In the case of the alcohols, the BDEs obtained from experiment and G3-RAD calculations increase significantly with increasing alkylation, whereas B3-LYP predicts that the relative BDEs remain close to zero. In the case of the ethers, G3-RAD and experiment predict an increase in the BDEs for Me to *i*-Pr followed by a small decrease for *t*-Bu, whereas B3-LYP predicts a significant decrease in going from R = Me to R = *t*-Bu. This problem had not been noted in the earlier study by Chen and Bozzelli[10] because, as explained above, the BDEs were not calculated directly but instead obtained via an isodesmic method that allowed for substantial cancellation of error. Although this highlights the potential value of an isodesmic approach for obtaining useful results from low-level calculations, it depends on the availability of reliable data for the relevant reference reactions and is not a general solution to the problem of predicting relative BDEs.

This failure of B3-LYP to predict even the correct *relative* values of the BDEs in some instances is of concern, as it threatens to undermine not only efforts to measure reliable absolute values of bond energies and hydrogen-abstraction enthalpies via this method but also efforts to study competing mechanistic pathways and to measure and rationalize the effects of substituents on BDEs and abstraction reactions in a wider context. It is thus desirable to try to identify a reliable alternative low-cost method for the calculation of BDEs. During the course of our earlier work, we noted that restricted (open-shell) second-order Møller−Plesset perturbation theory (RMP2), if applied with a triple-ζ basis set, showed larger errors than B3-LYP in the calculation of heats of formation and absolute BDEs, but performed reasonably well in the prediction of relative BDEs (see Figure 1c).[11] However, the behavior is by no means perfect, and the RMP2 method suffers from two additional disadvantages: (a) it is considerably more expensive than DFT procedures, and (b) it is not as accurate as the best DFT methods for the prediction of barrier heights in hydrogen abstraction.[9] It is thus of interest to examine the performance of alternative low-cost methods.

In the present work, we examine the performance of a wide range of pure and hybrid DFT methods for the calculation of absolute and relative R−X BDEs (R = Me, Et, *i*-Pr, *t*-Bu; X = H, CH$_3$, OCH$_3$, OH, F) with a view to identifying low-cost methods capable of reproducing the correct qualitative trends in these data. In particular, we include in our study a number of "new generation" hybrid DFT methods, including KMLYP,[16] B1B95,[17] MPW1PW91,[18] MPW1B95,[19] BB1K,[2] MPW1K,[20] MPWB1K,[19] and BMK.[21] Recent studies have suggested that a number of these methods show very good performance for both the kinetics and thermodynamics of chemical reactions,[19,21] and it is of interest to see how well they perform in these problematic systems. Because the RMP2 method proved promising in our earlier study, we also examine its performance with a wider range of basis sets. We also consider two recent modifications of MP2 theory, namely spin-component-scaled MP2 (SCS-MP2)[22] and scaled-opposite-spin MP2 (SOS-MP2).[23] These two methods have been found to provide improved performance compared with the standard MP2 method,[22,23] and it is of interest to examine how they fare in these problem systems.

2. Theoretical Procedures

Standard ab initio molecular orbital theory and density functional theory (DFT) calculations were carried out using the GAUSSIAN 03,[24] MOLPRO 2002.3[25] and ACESII 3.0[26] programs. Bond dissociation energies at 0 K were calculated for a series of R−X molecules (R = Me, Et, *i*-Pr and *t*-Bu, and X = H, CH$_3$, OCH$_3$, OH and F), with a view to examining the effect of level of theory on the accuracy of the results. To allow for a consistent comparison between the various methods, all geometries were optimized with B3-LYP/6-31G(d) and all corrections for the zero-point vibrational energies were calculated using scaled[27] B3-LYP/6-31G(d) frequencies. Improved relative energies were then calculated using a range of methods including various DFT- and MP2-based methods, as well as G3(MP2)-RAD and G3-RAD. All DFT calculations were carried out using unrestricted wave functions, whereas calculations at the MP2-based levels of theory (i.e., RMP2, SCS-MP2 and SOS-MP2) used restricted wave functions.

The DFT calculations were performed using the 6-311+G-(3df,2p) basis set and a variety of different functionals. These include a traditional pure functional, B-LYP, hybrid 3-parameter functionals, B3-LYP and B3-P86, and a number of relatively new functionals, including KMLYP,[16] B1B95,[17] MPW1PW91,[18] MPW1B95,[19] BB1K,[2] MPW1K,[20] MPWB1K,[19] and BMK.[21] These latter functionals have been specifically optimized to give improved performance for studying the thermodynamics and/or kinetics of chemical reactions. KMLYP is a hybrid 2-parameter functional in which the exchange functional is a mixture of Slater exchange and exact exchange (55.7%). This method differs from the other DFT methods in that it includes an additional empirical correction term, somewhat analogous to the higher-level correction (HLC) term in the G3-based methods, which depends on the number of unpaired electrons and the number of lone pairs. The hybrid MPW1PW91 (also known as mPW1PW91) functional is based on the modified exchange and correlation functionals proposed by Perdew and Wang in 1991. The MPW1K method was obtained by reoptimizing the fraction of HF exchange in the MPW1PW91 functional, to improve its prediction of barrier heights for a test set of hydrogen-atom-abstraction reactions.[20] The remaining functionals fall into the category of hybrid meta-GGA functionals, which depend on the kinetic energy density. B1B95 is a hybrid version of Becke's BB95 functional,[28] whereas the BB1K model is the same

functional but with the fraction of HF exchange reoptimized for the prediction of kinetics.[2] MPW1B95 and MPWB1K both comprise the modified Perdew and Wang 1991 exchange functional and Becke's 1995 meta correlation functional, the difference being that the former was optimized for thermochemistry, whereas the latter was optimized for kinetics.[19] The BMK functional is somewhat different to the others, as it simulates a variable exact exchange. This is achieved by the combination of exact exchange (42%) and terms depending on the kinetic energy density. This combination is intended to lead to a "back-correction" for excessive HF exchange in systems where that would be undesirable.[21]

The RMP2 relative energies were computed with the 6-311+G-(3df,2p), cc-pVTZ and cc-pVQZ basis sets. The calculations with the cc-pVTZ and cc-pVQZ basis sets were also used for two-point extrapolations to the infinite-basis-set limit (denoted here as ∞Z), using n^{-5} for the SCF component and n^{-3} for the correlation energy component.[29] In addition to standard RMP2, two recent modifications of second-order Møller−Plesset theory, namely spin-component-scaled MP2 (SCS-MP2)[22] and scaled-opposite-spin MP2 (SOS-MP2),[23] were also employed. These two methods were introduced to provide an improvement over the performance of standard MP2, and initial testing has produced very promising results.[22,23] Both methods are based on the idea that the correlation energy (E_c) can be split into two components:

$$E_c = E_S + E_T \qquad (3)$$

where E_S is the contribution from opposite-spin electron pairs, whereas same-spin electron pairs contribute to E_T. The original idea by Grimme[22] was to approximate the correlation energy by applying separate scaling factors for the two contributions:

$$E_c \approx p_S E_S + p_T E_T \qquad (4)$$

The scaling factors ($p_S = {}^6/_5$ and $p_T = {}^1/_3$) were obtained through fitting to experimental enthalpies of formation but justified theoretically in a qualitative manner. The SOS-MP2 method of Head-Gordon and co-workers[23] simplifies the SCS-MP2 splitting scheme by including the opposite-spin components only. A slightly larger scaling factor $p_S = 1.3$ is used to compensate for the absence of explicit same-spin correlation. If implemented in an efficient way, SOS-MP2 offers the possibility of significantly reduced computational cost for larger systems (compared with standard MP2), as it is possible to formulate it as a fourth-order (rather than fifth-order) method.[23] Both modifications of the standard MP2 method have proven to work well for the prediction of enthalpies and barrier heights for a variety of chemical systems and give accuracy comparable to that of QCISD(T).[22,23,30]

To assist in the interpretation of the BDE results, the heats of formation at 0 K for the radical (R•) and closed-shell (R−X) species were also calculated at the levels of theory mentioned above. The heats of formation were obtained from the calculated total atomization energies, together with reliable experimental values for the heats of formation of the constituent atoms at 0 K, using the procedure outlined by Nicolaides et al.[31] Where possible, the calculated values are compared with the corresponding gas-phase experimental data.[32] In cases where only the 298 K experimental values are available, these have been back-corrected to 0 K by subtracting the B3-LYP/6-31G(d) temperature corrections.

3. Results and Discussion

The heats of formation (ΔH_f, 0 K, kJ mol^{-1}) of the R−X and R• species (R = Me, Et, *i*-Pr and *t*-Bu; X = H, CH$_3$, OCH$_3$,

TABLE 1: Heats of Formation (kJ mol^{-1}, 0 K)^a

Method^b	R−H				R−CH$_3$				R−OCH$_3$			
	R = Me	R = Et	R = *i*-Pr	R = *t*-Bu	R = Me	R = Et	R = *i*-Pr	R = *t*-Bu	R = Me	R = Et	R = *i*-Pr	R = *t*-Bu
B-LYP	−52.6	−34.9	−25.2	−18.8	−34.9	−25.2	−18.8	−9.9	−147.9	−152.2	−150.0	−141.0
B3-LYP	−68.9	−63.8	−67.1	−74.3	−63.8	−67.1	−74.3	−79.7	−161.4	−178.7	−190.1	−195.5
B3-P86	−121.1	−164.0	−215.9	−272.6	−164.0	−215.9	−272.6	−328.7	−280.4	−346.1	−406.9	−463.3
KMLYP	−68.9	−76.5	−94.8	−119.8	−76.5	−94.8	−119.8	−143.7	−180.0	−212.6	−241.8	−268.5
B1B95	−54.3	−51.1	−56.8	−67.5	−51.1	−56.8	−67.5	−78.9	−155.8	−176.8	−193.1	−205.7
MPW1PW91	−48.7	−48.7	−57.6	−71.2	−48.7	−57.6	−71.2	−83.6	−145.6	−169.6	−188.5	−202.7
MPW1B95	−58.2	−59.4	−70.0	−86.2	−59.4	−70.0	−86.2	−102.2	−211.9	−236.3	−256.7	−273.9
BB1K	−75.2	−92.6	−119.1	−150.8	−92.6	−119.1	−150.8	−182.3	−241.3	−281.5	−317.3	−349.8
MPW1K	−74.7	−100.3	−134.9	−174.3	−100.3	−134.9	−174.3	−213.0	−240.1	−288.2	−331.4	−370.3
MPWB1K	−78.3	−99.8	−130.8	−167.6	−99.8	−130.8	−167.6	−204.5	−243.6	−288.4	−329.2	−367.2
BMK	−63.2	−66.9	−80.4	−100.1	−66.9	−80.4	−100.1	−119.5	−175.8	−202.5	−225.9	−247.1
RMP2	−13.8	3.7	7.3	0.3	3.7	7.3	0.3	−11.7	−116.7	−126.6	−137.1	−149.4
RMP2/cc-pVTZ	−25.1	−12.7	−12.7	−22.0	−12.7	−12.7	−22.0	−35.5	−118.9	−133.0	−146.3	−160.2
SCS-MP2/cc-pVTZ	−40.2	−25.0	−20.6	−23.9	−25.0	−20.6	−23.9	−30.0	−118.3	−127.7	−134.8	−141.2
SOS-MP2/cc-pVTZ	−47.7	−31.1	−24.5	−24.8	−31.1	−24.5	−24.8	−27.2	−118.0	−125.1	−129.0	−131.7
RMP2/cc-pVQZ	−43.5	−45.8	−60.9	−85.3	−45.8	−60.9	−85.3	−113.8	−165.9	−194.6	−222.7	−251.3
SCS-MP2/cc-pVQZ	−61.2	−62.4	−74.7	−94.8	−62.4	−74.7	−94.8	−117.4	−170.1	−195.8	−219.3	−242.0
SOS-MP2/cc-pVQZ	−70.1	−70.7	−81.7	−99.5	−70.7	−81.7	−99.5	−119.2	−172.2	−196.5	−217.6	−237.4
RMP2/∞Z	−56.3	−68.7	−94.1	−129.0	−68.7	−94.1	−129.0	−167.8	−197.7	−236.6	−275.0	−313.9
SCS-MP2/∞Z	−75.8	−88.4	−112.3	−144.0	−88.4	−112.3	−144.0	−178.1	−205.4	−242.6	−277.6	−311.8
SOS-MP2/∞Z	−85.6	−98.3	−121.4	−151.5	−98.3	−121.4	−151.5	−183.3	−209.3	−245.6	−278.9	−310.7
G3(MP2)-RAD	−65.3	−66.8	−80.9	−103.9	−66.8	−80.9	−103.9	−130.7	−165.4	−193.5	−220.9	−248.7
G3-RAD	−65.6	−67.6	−81.7	−104.9	−67.6	−81.7	−104.9	−132.7	−166.7	−195.0	−223.1	−251.8
Experiment^c	−66.9	−67.9	−82.0	−105.1	−67.9	−82.0	−105.1	−	−166.0	−192.0	−221.5	−246.7

Method^b	R−OH				R−F				R				MAD^d	MD^d
	R = Me	R = Et	R = *i*-Pr	R = *t*-Bu	R = Me	R = Et	R = *i*-Pr	R = *t*-Bu	R = Me	R = Et	R = *i*-Pr	R = *t*-Bu		
B-LYP	−184.8	−188.9	−193.6	−194.2	−228.9	−238.1	−248.0	−254.0	151.5	147.0	139.7	133.3	48.3	48.2
B3-LYP	−187.3	−204.4	−222.3	−237.2	−230.1	−252.1	−275.3	−295.3	139.7	124.7	105.8	87.2	18.5	16.5
B3-P86	−261.4	−326.6	−393.7	−458.7	−287.2	−356.9	−428.7	−498.3	98.4	34.8	−32.9	−101.0	130.7	−130.7
KMLYP	−195.4	−227.6	−262.8	−297.3	−240.6	−276.8	−316.7	−355.4	145.9	119.7	87.6	53.6	14.0	−14.0
B1B95	−180.8	−201.3	−223.7	−244.2	−227.8	−252.8	−279.9	−304.8	158.5	140.8	119.0	96.6	21.3	21.3
MPW1PW91	−169.2	−192.7	−218.2	−241.2	−217.0	−245.2	−275.4	−303.1	150.7	131.1	106.9	82.0	22.6	22.8
MPW1B95	−233.6	−257.6	−283.9	−308.7	−230.6	−259.1	−290.0	−319.1	157.2	135.3	108.9	81.5	18.2	−5.9
BB1K	−247.8	−287.6	−329.4	−369.7	−234.8	−278.9	−325.3	−370.0	137.8	100.8	59.4	16.9	48.9	−48.9
MPW1K	−240.4	−288.2	−337.8	−385.5	−224.8	−277.0	−331.3	−383.7	124.0	80.3	31.6	−18.0	61.1	−60.8
MPWB1K	−245.7	−289.9	−336.7	−382.3	−239.3	−288.0	−339.3	−389.2	136.2	95.3	49.5	2.3	58.6	−58.6
BMK	−193.0	−219.3	−248.7	−277.3	−233.7	−263.6	−297.0	−329.8	151.5	130.0	103.4	75.0	4.0	−0.1
RMP2	−159.3	−167.7	−182.7	−201.5	−211.3	−221.7	−239.4	−260.7	187.5	191.2	185.3	173.3	70.3	70.3
RMP2/cc-pVTZ	−157.6	−170.8	−189.1	−209.6	−207.2	−222.7	−243.2	−265.9	180.7	179.8	170.4	155.8	59.8	59.8
SCS-MP2/cc-pVTZ	−157.7	−166.3	−178.7	−192.5	−202.8	−214.0	−229.1	−245.5	171.0	173.8	169.2	160.6	61.9	61.9
SOS-MP2/cc-pVTZ	−157.7	−164.1	−173.6	−183.9	−200.6	−209.6	−222.1	−235.3	166.1	170.8	168.6	163.0	62.9	62.9
RMP2/cc-pVQZ	−192.0	−219.8	−252.7	−287.9	−233.3	−263.0	−298.3	−335.9	166.1	150.4	125.1	95.4	11.3	8.6
SCS-MP2/cc-pVQZ	−195.4	−220.3	−249.0	−278.9	−230.7	−257.9	−289.5	−322.4	154.1	140.1	118.6	93.2	6.4	5.0
SOS-MP2/cc-pVQZ	−197.0	−220.6	−247.2	−274.5	−229.5	−255.4	−285.1	−315.6	148.7	135.9	115.4	92.1	5.8	3.2
RMP2/∞Z	−214.8	−252.8	−295.9	−341.4	−250.5	−290.3	−336.0	−384.1	155.6	129.1	94.1	53.9	27.8	−26.5
SCS-MP2/∞Z	−220.5	−256.9	−297.1	−338.4	−249.4	−287.9	−331.0	−375.5	142.6	116.9	83.7	46.6	34.2	−34.2
SOS-MP2/∞Z	−223.4	−259.0	−297.6	−337.0	−248.8	−286.6	−328.6	−371.3	136.1	110.8	78.5	43.0	38.0	−38.0
G3(MP2)-RAD	−189.2	−216.0	−248.2	−282.5	−228.0	−257.1	−292.0	−329.4	147.1	131.4	107.4	78.8	1.2	0.9
G3-RAD	−189.6	−216.7	−249.5	−284.7	−228.0	−257.7	−293.3	−331.7	148.9	132.3	107.6	77.7	0.0	0.0
Experiment^c	−189.8	−217.2	−248.1	−281.8	−226.6	−	−	−	149.8	131.7	106.8	74.5	−	−

^{a} Calculated using B3-LYP/6-31G(d) geometries and incorporating scaled zero-point vibrational energy corrections. ^{b} All DFT functionals are used in conjunction with the 6-311+G(3df,2p) basis set. If not stated otherwise, the 6-311+G(3df,2p) basis set is also used for RMP2. ^{c} Taken from ref 32 unless otherwise noted. Experimental values at 298 K back-corrected to 0 K using temperature corrections obtained at the B3-LYP/6-31G(d) level. Experimental results for the radicals are taken from ref 33. ^{d} MD and MAD are respectively the mean deviations and mean absolute deviations from G3-RAD values. Note that the mean deviation and mean absolute deviation of G3-RAD from the experimental values are −0.5 and +1.3 kJ mol^{-1}, respectively.

OH, F) at a variety of levels of theory are shown in Table 1. The corresponding gas-phase experimental values[32,33] are also included in Table 1 for purposes of comparison. The absolute (Table 2) and relative (Table 3) R−X bond dissociation energies (BDEs) were also calculated. For the purposes of the present work, the relative BDE of a species R−X is defined as the difference between the R−X BDE and the corresponding Me−X BDE (at the same level of theory). To assist in the qualitative analysis of the results, the relative BDEs are plotted as a function of the R-group for each of the R−X series in Figure 2.

Heats of Formation. Examining the heats of formation in Table 1, we note that there is generally excellent agreement between the high-level G3-RAD values and the corresponding experimental values. The mean absolute deviation from the available experimental values is just 1.3 kJ mol^{-1}, the maximum deviation (which occurs for *t*-Bu-OCH$_3$) is only 5.1 kJ mol^{-1} and the majority of results agree to within 1 kJ mol^{-1}. On the basis of this excellent performance, we treat the G3-RAD values as our benchmark for the remainder of this study. The mean absolute deviations (MADs) and mean deviations (MDs) from the corresponding G3-RAD values at each level of theory are included in Tables 1 and 2. We note to begin that the (slightly) less-computationally intensive G3(MP2)-RAD method shows excellent agreement with G3-RAD (MAD 1.2 kJ mol^{-1}) and

TABLE 2: Bond Dissociation Energies (kJ mol⁻¹, 0 K)ᵃ

	R–H				R–CH₃				R–OCH₃			
Methodᵇ	R = Me	R = Et	R = i-Pr	R = t-Bu	R = Me	R = Et	R = i-Pr	R = t-Bu	R = Me	R = Et	R = i-Pr	R = t-Bu
B-LYP	420.1	397.9	380.9	368.1	337.8	323.6	309.9	294.6	304.1	303.9	294.4	279.0
B3-LYP	424.6	404.5	389.0	377.6	343.1	331.4	319.8	306.6	310.3	312.6	305.1	292.0
B3-P86	435.6	414.9	399.0	387.7	360.9	349.2	338.1	326.1	328.9	331.0	324.1	312.5
KMLYP	430.9	412.2	398.5	389.4	368.4	360.5	353.4	343.2	335.8	342.1	339.3	331.9
B1B95	428.9	407.9	391.9	380.2	368.2	356.2	345.1	334.0	332.3	335.5	330.0	320.3
MPW1PW91	415.5	395.8	380.5	369.3	350.2	339.4	328.8	316.4	317.8	322.1	316.8	306.2
MPW1B95	431.4	410.7	395.0	383.7	373.7	362.5	352.3	340.9	336.3	338.8	332.8	322.6
BB1K	429.1	409.5	394.5	383.8	368.2	357.8	348.0	337.1	328.9	332.1	326.5	316.6
MPW1K	414.7	396.6	382.5	372.4	348.2	339.1	329.9	318.9	311.1	315.6	310.1	299.4
MPWB1K	430.5	411.1	396.3	385.9	372.2	362.3	353.3	343.0	333.4	337.2	332.3	323.1
BMK	430.8	413.0	399.8	391.1	369.9	362.0	355.0	346.0	336.4	341.6	338.3	331.2
RMP2	417.4	403.5	394.0	389.0	371.3	371.4	372.6	372.5	370.3	383.9	388.5	388.8
RMP2/cc-pVTZ	421.8	408.5	399.2	393.8	374.1	373.3	373.1	372.0	368.3	381.5	385.4	384.7
SCS-MP2/cc-pVTZ	427.1	414.8	405.9	400.5	366.9	365.4	364.1	361.5	354.3	366.6	369.1	366.9
SOS-MP2/cc-pVTZ	429.8	417.9	409.2	403.8	363.3	361.4	359.5	356.3	347.4	359.1	360.9	358.0
RMP2/cc-pVQZ	425.2	411.5	402.1	396.7	377.3	376.4	376.2	374.9	374.5	387.2	390.7	389.6
SCS-MP2/cc-pVQZ	431.2	418.4	409.3	403.9	370.7	368.9	367.5	364.7	360.8	372.5	374.5	371.8
SOS-MP2/cc-pVQZ	434.3	421.9	413.1	407.6	367.3	365.2	363.2	359.6	353.9	365.1	366.4	362.9
RMP2/∞Z	428.0	413.9	404.2	398.9	380.0	378.9	378.7	377.3	378.9	391.3	394.6	393.4
SCS-MP2/∞Z	434.5	421.3	412.1	406.6	373.7	371.8	370.3	367.3	365.3	376.7	378.6	375.6
SOS-MP2/∞Z	437.8	425.1	416.0	410.5	370.6	368.3	366.2	362.4	358.5	369.4	370.5	366.7
G3(MP2)-RAD	428.4	414.3	404.4	398.7	361.0	359.4	358.4	356.6	340.3	352.6	356.1	355.2
G3-RAD	430.6	415.9	405.3	398.6	365.4	362.9	361.4	359.3	343.6	355.3	358.7	357.5
Experimentᶜ	432.6	415.6	404.8	395.6	367.4	363.5	361.6	356.1	340.5	348.5	353.0	345.9

	R–OH				R–F					
Methodᵇ	R = Me	R = Et	R = i-Pr	R = t-Bu	R = Me	R = Et	R = i-Pr	R = t-Bu	MADᵈ	MDᵈ
B-LYP	360.9	360.6	357.9	352.2	457.7	462.5	465.0	464.7	33.1	−32.8
B3-LYP	358.5	360.6	359.7	355.9	447.1	454.2	458.5	460.0	29.0	−29.0
B3-P86	377.8	379.4	378.8	375.6	463.0	469.1	473.2	474.7	14.5	−12.6
KMLYP	374.9	380.8	384.0	384.4	463.9	473.9	481.7	486.4	8.1	−5.8
B1B95	380.8	383.5	384.2	382.3	463.7	471.0	476.3	478.8	12.2	−10.0
MPW1PW91	363.9	367.8	369.0	367.2	445.2	453.7	459.6	462.5	25.2	−25.2
MPW1B95	383.2	385.3	385.3	382.6	465.2	471.8	476.3	478.1	10.5	−7.1
BB1K	372.4	375.3	375.6	373.5	450.0	457.2	462.1	464.4	14.7	−14.4
MPW1K	351.8	355.8	356.9	354.9	426.2	434.6	440.4	443.1	32.4	−32.4
MPWB1K	376.0	379.4	380.4	378.8	453.0	460.7	466.2	469.0	11.2	−10.3
BMK	380.4	385.2	387.9	388.1	462.6	471.0	477.7	482.2	7.4	−5.0
RMP2	396.9	409.0	418.2	424.9	476.2	490.3	502.2	511.4	19.7	15.1
RMP2/cc-pVTZ	391.6	403.8	412.7	418.7	465.3	479.9	491.0	499.1	15.1	12.3
SCS-MP2/cc-pVTZ	377.8	389.2	397.1	402.2	451.2	465.1	475.7	483.5	4.3	2.7
SOS-MP2/cc-pVTZ	370.9	382.0	389.3	394.0	444.1	457.8	468.1	475.7	4.3	−2.1
RMP2/cc-pVQZ	399.1	410.9	419.2	424.6	476.4	490.1	500.8	508.7	19.6	18.1
SCS-MP2/cc-pVQZ	385.6	396.5	403.8	408.3	462.3	475.4	485.5	492.9	8.7	8.7
SOS-MP2/cc-pVQZ	378.9	389.4	396.1	400.1	455.2	468.0	477.9	485.1	4.2	4.0
RMP2/∞Z	404.3	415.9	423.9	429.1	483.6	496.9	507.4	515.3	22.7	22.2
SCS-MP2/∞Z	391.0	401.7	408.6	412.8	469.4	482.1	492.2	499.5	13.0	13.0
SOS-MP2/∞Z	384.3	394.5	401.0	404.7	462.3	474.8	484.5	491.6	8.4	8.4
G3(MP2)-RAD	370.6	381.7	389.9	395.6	452.5	465.8	476.9	485.7	2.4	−2.3
G3-RAD	374.2	384.7	392.8	398.1	454.3	467.3	478.2	486.8	0.0	0.0
Experimentᶜ	378.5	387.8	393.8	395.2	453.7	−	−	−	−	−

ᵃ Calculated using B3-LYP/6-31G(d) geometries and incorporating scaled zero-point vibrational energy corrections. ᵇ All DFT functionals are used in conjunction with the 6-311+G(3df,2p) basis set. If not stated otherwise, the 6-311+G(3df,2p) basis set is also used for RMP2. ᶜ Calculated using the experimental heats of formation in Table 1, in conjunction with the following additional values (0 K, kJ mol⁻¹) from ref 32: −131.8 (neopentane), 38.8 (•OH), 24.7 (•OCH₃), 77.4 (•F), and 216.0 (•H). ᵈ MD and MAD are respectively the mean deviations and mean absolute deviations from G3-RAD values. Note that the mean deviation and mean absolute deviation of G3-RAD from the experimental values are 1.4 and 3.0 kJ mol⁻¹, respectively.

could serve as a substitute for G3-RAD in larger systems. These results reinforce those of previous studies in which the G3-(MP2)-RAD and G3-RAD methods were shown to provide chemical accuracy for the heats of formation of various open- and closed-shell species,[34] radical stabilization energies,[8] and the thermodynamics of a variety of radical reactions.[9,11,35,36] Although these composite methods provide a cost-effective compromise between accuracy and economy, they nonetheless remain computationally intensive procedures. Even the G3-(MP2)-RAD method is only practical with our existing resources for systems of up to approximately 15 non-hydrogen atoms. It

is thus important to try to identify suitable lower-cost procedures that might be applicable to larger systems. For this reason, we now examine the performance of the DFT- and MP2-based methods.

If we consider first the DFT methods, we note that the pure DFT method (B-LYP) fails comprehensively to reproduce the correct qualitative trends in the heats of formation. At the G3-RAD level, the heat of formation decreases substantially with increasing alkylation of R for all of the R–X and R• systems. However, at the B-LYP level this decrease in the heat of formation is greatly diminished for R–OH, R–F and R•, and

Trends in R−X Bond Dissociation Energies

J. Phys. Chem. A, Vol. 109, No. 33, 2005 **7563**

TABLE 3: Relative Bond Dissociation Energies (kJ mol⁻¹, 0 K)ᵃ

	R−H				R−CH₃				R−OCH₃			
Method	R = Me	R = Et	R = i-Pr	R = t-Bu	R = Me	R = Et	R = i-Pr	R = t-Bu	R = Me	R = Et	R = i-Pr	R = t-Bu
B-LYP	0.0	−22.2	−39.2	−52.0	0.0	−14.2	−27.9	−43.2	0.0	−0.2	−9.7	−25.1
B3-LYP	0.0	−20.1	−35.6	−47.0	0.0	−11.7	−23.3	−36.5	0.0	2.3	−5.2	−18.3
B3-P86	0.0	−20.7	−36.6	−47.9	0.0	−11.7	−22.8	−34.8	0.0	2.1	−4.8	−16.4
KMLYP	0.0	−18.7	−32.4	−41.5	0.0	−7.9	−15.0	−25.2	0.0	6.3	3.5	−3.9
B1B95	0.0	−21.0	−37.0	−48.7	0.0	−12.0	−23.1	−34.2	0.0	3.2	−2.3	−12.0
MPW1PW91	0.0	−19.7	−35.0	−46.2	0.0	−10.7	−21.3	−33.8	0.0	4.3	−1.0	−11.6
MPW1B95	0.0	−20.7	−36.4	−47.7	0.0	−11.2	−21.4	−32.8	0.0	2.5	−3.5	−13.7
BB1K	0.0	−19.6	−34.6	−45.3	0.0	−10.4	−20.2	−31.1	0.0	3.2	−2.4	−12.3
MPW1K	0.0	−18.1	−32.2	−42.3	0.0	−9.1	−18.3	−29.3	0.0	4.5	−1.0	−11.7
MPWB1K	0.0	−19.4	−34.2	−44.6	0.0	−9.9	−18.9	−29.2	0.0	3.8	−1.1	−10.3
BMK	0.0	−17.8	−31.0	−39.7	0.0	−7.9	−14.9	−23.9	0.0	5.2	1.9	−5.2
RMP2	0.0	−13.8	−23.3	−28.3	0.0	0.1	1.3	1.1	0.0	13.6	18.3	18.5
RMP2/cc-pVTZ	0.0	−13.3	−22.6	−27.9	0.0	−0.8	−0.9	−2.1	0.0	13.2	17.1	16.4
SCS-MP2/cc-pVTZ	0.0	−12.3	−21.2	−26.6	0.0	−1.5	−2.8	−5.4	0.0	12.3	14.8	12.6
SOS-MP2/cc-pVTZ	0.0	−11.9	−20.6	−26.0	0.0	−1.9	−3.7	−7.0	0.0	11.8	13.6	10.6
RMP2/cc-pVQZ	0.0	−13.7	−23.2	−28.6	0.0	−1.0	−1.2	−2.4	0.0	12.7	16.2	15.1
SCS-MP2/cc-pVQZ	0.0	−12.8	−21.9	−27.3	0.0	−1.8	−3.2	−6.0	0.0	11.7	13.7	11.0
SOS-MP2/cc-pVQZ	0.0	−12.4	−21.3	−26.8	0.0	−2.1	−4.1	−7.7	0.0	11.2	12.5	9.0
RMP2/∞Z	0.0	−14.1	−23.8	−29.1	0.0	−1.1	−1.3	−2.7	0.0	12.4	15.7	14.5
SCS-MP2/∞Z	0.0	−13.2	−22.5	−27.9	0.0	−1.9	−3.4	−6.4	0.0	11.4	13.3	10.3
SOS-MP2/∞Z	0.0	−12.7	−21.8	−27.3	0.0	−2.3	−4.4	−8.2	0.0	10.9	12.0	8.2
G3(MP2)-RAD	0.0	−14.1	−24.0	−29.7	0.0	−1.6	−2.6	−4.4	0.0	12.3	15.8	14.9
G3-RAD	0.0	−14.7	−25.3	−32.0	0.0	−2.5	−4.0	−6.1	0.0	11.7	15.1	13.9
Experiment	0.0	−17.0	−27.8	−37.0	0.0	−3.9	−5.8	−11.3	0.0	8.0	12.5	5.4

	R−OH				R−F			
Method	R = Me	R = Et	R = i-Pr	R = t-Bu	R = Me	R = Et	R = i-Pr	R = t-Bu
B-LYP	0.0	−0.3	−3.0	−8.7	0.0	4.8	7.3	7.0
B3-LYP	0.0	2.1	1.2	−2.6	0.0	7.1	11.4	12.9
B3-P86	0.0	1.6	1.0	−2.2	0.0	6.1	10.2	11.7
KMLYP	0.0	5.9	9.1	9.5	0.0	10.0	17.8	22.5
B1B95	0.0	2.8	3.4	1.5	0.0	7.3	12.5	15.1
MPW1PW91	0.0	3.9	5.1	3.3	0.0	8.5	14.5	17.4
MPW1B95	0.0	2.1	2.1	−0.6	0.0	6.6	11.1	12.9
BB1K	0.0	2.9	3.2	1.1	0.0	7.2	12.1	14.4
MPW1K	0.0	4.0	5.1	3.1	0.0	8.4	14.2	16.9
MPWB1K	0.0	3.4	4.4	2.8	0.0	7.7	13.2	16.0
BMK	0.0	4.8	7.5	7.7	0.0	8.4	15.1	19.6
RMP2	0.0	12.2	21.3	28.0	0.0	14.1	26.0	35.2
RMP2/cc-pVTZ	0.0	12.3	21.2	27.1	0.0	14.6	25.7	33.8
SCS-MP2/cc-pVTZ	0.0	11.4	19.3	24.4	0.0	13.9	24.5	32.3
SOS-MP2/cc-pVTZ	0.0	11.0	18.4	23.0	0.0	13.7	24.1	31.6
RMP2/cc-pVQZ	0.0	11.8	20.1	25.5	0.0	13.7	24.4	32.2
SCS-MP2/cc-pVQZ	0.0	10.9	18.2	22.7	0.0	13.1	23.2	30.6
SOS-MP2/cc-pVQZ	0.0	10.5	17.2	21.2	0.0	12.9	22.7	29.9
RMP2/∞Z	0.0	11.5	19.6	24.8	0.0	13.3	23.9	31.7
SCS-MP2/∞Z	0.0	10.7	17.6	21.9	0.0	12.7	22.8	30.1
SOS-MP2/∞Z	0.0	10.2	16.7	20.4	0.0	12.5	22.2	29.3
G3(MP2)-RAD	0.0	11.1	19.3	25.0	0.0	13.3	24.4	33.2
G3-RAD	0.0	10.5	18.6	23.9	0.0	13.0	23.9	32.5
Experiment	0.0	9.3	15.3	16.7	−	−	−	−

ᵃ Calculated from the BDEs in Table 2.

actually reversed for R−H, R−CH₃ and R−OCH₃. This demonstrates the importance of the inclusion of exact Hartree−Fock (HF) exchange. The rest of the functionals include a portion of exact exchange that varies from 20% in B3-LYP to 55.7% in KMLYP, and all of these functionals succeed in predicting the correct trends in the heats of formation. However, with the exception of BMK, and to a lesser extent KMLYP and MPW1B95, none of these functionals reproduce the absolute values adequately. Indeed in some cases, such as B3-P86, these methods overestimate ΔH_f by more than 200 kJ mol⁻¹. In general terms, the functionals optimized for thermodynamics (such as B1B95, MPW1PW91 and B3-LYP) tend to overestimate heats of formation (MDs of 16.5 to 22.8 kJ mol⁻¹), whereas the functionals optimized for kinetics (such as BB1K, MPW1K and MPWB1K) tend to underestimate them (MDs of

−60.8 to −48.9 kJ mol⁻¹). KMLYP, also optimized for kinetics, also systematically underestimates the heats of formation (MD of −14.0 kJ mol⁻¹) but has a reasonably low MAD (14.0 kJ mol⁻¹). However, this is primarily achieved through the use of a higher-level correction term, the uncorrected KMLYP method significantly underestimating the heats of formation (MD of −179.4 kJ mol⁻¹). In contrast to the other DFT methods, the BMK functional performs remarkably well in predicting the absolute values of heats of formation. The mean absolute deviation (MAD) for this method is just 4 kJ mol⁻¹ and the maximum deviation (which occurs for t-Bu−CH₃) is reasonably small (at 13.2 kJ mol⁻¹). It would appear that the simulated variable exchange in BMK succeeds in achieving an accurate description of the heats of formation, at least for the systems examined in the present study.
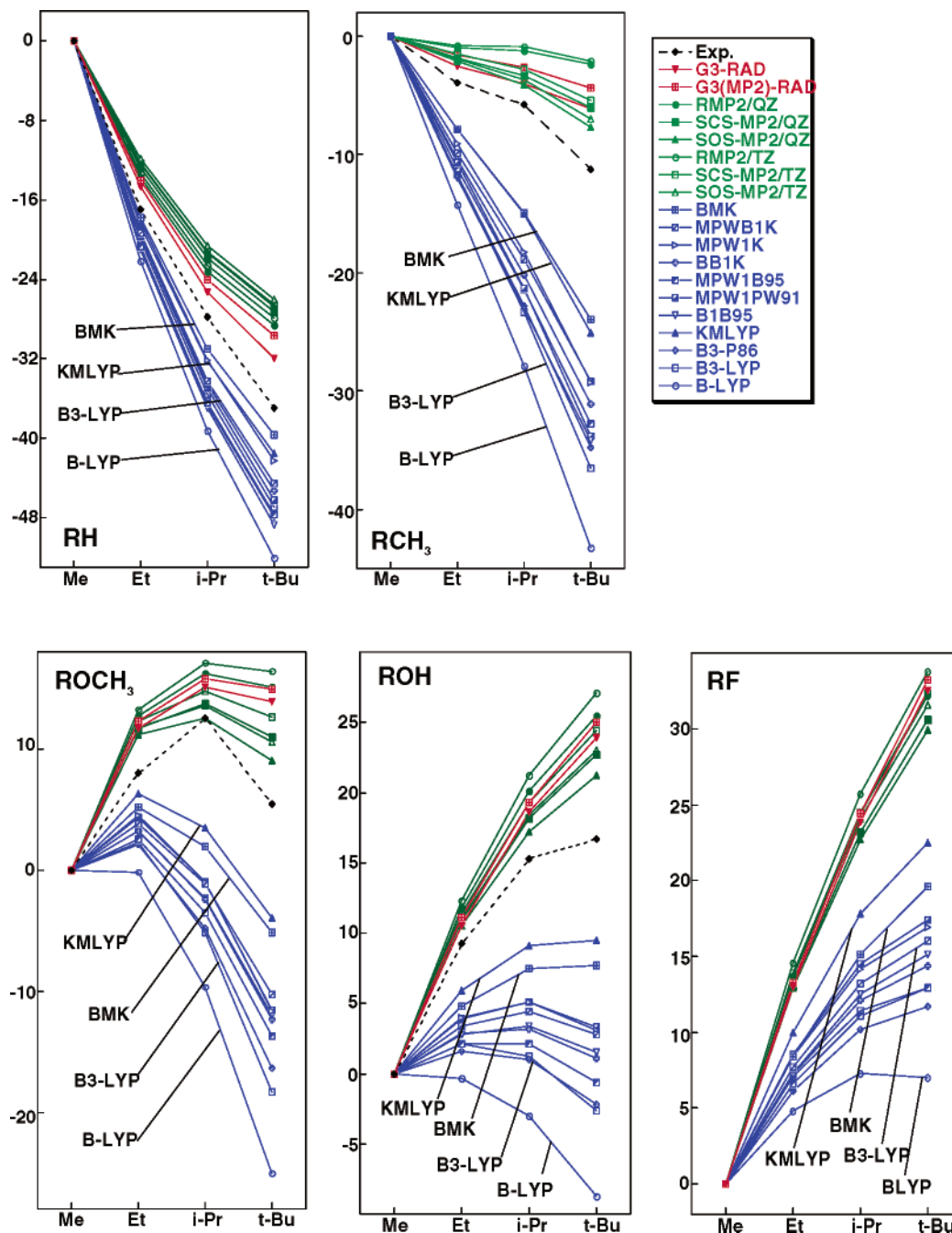
Figure 2. Effect of level of theory on the relative bond dissociation energies (kJ mol^{-1}) for R−X species (R = Me, Et, *i*-Pr, *t*-Bu; X = H, CH$_3$, OCH$_3$, OH, F).

Further examination of Table 1 shows that the MP2 methods can produce large errors in the prediction of the absolute heats of formation. When computed with the same basis set as the DFT methods, i.e., 6-311+G(3df,2p), standard RMP2 has an MAD of 70.3 kJ mol^{-1}. This error is slightly diminished with the cc-pVTZ basis set (59.8 kJ mol^{-1}), and further reduced to 11.3 kJ mol^{-1} with cc-pVQZ. In fact, at this level, the errors for the polar systems (R−F, R−OH, and R−OCH$_3$) are very small, whereas those for the less polar systems (R−H, R−CH$_3$ and R•) are reasonably systematic, the heats of formation being overestimated by approximately 20 kJ mol^{-1}. This slow basis set convergence of MP2 (and indeed other ab initio correlated methods) is well-known, with convergence typically not achieved until the QZ or 5Z level.[37] If we use the cc-pVTZ and cc-pVQZ basis set values to extrapolate to the infinite-basis-set limit, the heats of formation decrease. Although the errors for many of

the nonpolar systems are further reduced as a consequence, those for the polar systems start to increase again. This leads to overall errors that are larger, with the infinite-basis-set RMP2 results underestimating the heats of formation (MD = −26.5 kJ mol^{-1}). Standard RMP2 is thus not very suitable for the accurate calculation of the absolute heats of formation for these systems.

The SCS-MP2 and SOS-MP2 results are also strongly basis-set dependent. In the case of SCS-MP2, the MAD for the cc-pVTZ calculations is 61.9 kJ mol^{-1} and this reduces to 6.4 kJ mol^{-1} with the QZ basis set. For SOS-MP2, the corresponding MADs are 62.9 and 5.8 kJ mol^{-1} with the TZ and QZ basis sets, respectively. In general, SCS-MP2 and SOS-MP2 show performance similar to standard MP2 for the heats of formation of the present systems. The MADs are marginally larger than for the corresponding MP2 calculations with the cc-pVTZ basis but around 4−6 kJ mol^{-1} smaller with the cc-pVQZ basis set.

Trends in R−X Bond Dissociation Energies

J. Phys. Chem. A, Vol. 109, No. 33, 2005 **7565**

As in the case of standard RMP2, when we extrapolate to an infinite basis set, the heats of formation decrease further and, as a result, the errors in the absolute heats of formation actually increase, the MDs for SCS-MP2 and SOS-MP2 being −34.2 and −38.0 kJ mol^{-1}, respectively. It thus appears that the small MADs in the cc-pVQZ calculations may be fortuitous. When the results are extrapolated to an infinite basis set, the new MP2 methods do not show better accuracy compared with standard MP2 for the calculation of the heats of formation in the present systems.

On the basis of these results, we conclude that the BMK method offers the best compromise between accuracy and expense for the calculation of absolute heats of formation for the systems examined.

Bond Dissociation Energies. If we consider next the bond dissociation energies (Table 2), we first note that G3-RAD again shows very good agreement with experiment. The MAD is just 3.0 kJ mol^{-1}, and in general the errors are less than 4 kJ mol^{-1}. The errors for the ethers R−OCH$_3$ are slightly larger than for the other systems. In particular, the *t*-Bu−OCH$_3$ BDE shows a deviation from the experimental value of 11.6 kJ mol^{-1}; however, even in this case, the error is only slightly larger than the total quoted experimental uncertainty (9 kJ mol^{-1}). As in the case of the heats of formation, the G3(MP2)-RAD BDEs show excellent agreement with the G3-RAD values (MAD 2.4 kJ mol^{-1}) and would serve as a suitable benchmark level of theory when G3-RAD calculations are impractical. Comparison with the experimental values in Figure 2 shows that, in general, both G3-RAD and G3(MP2)-RAD slightly underestimate the stabilizing effect on R−X BDEs of going from R = Me to *t*-Bu.

In general, the absolute errors at the lower levels of theory for the BDEs are much smaller than for the heats of formation due to a favorable cancellation of error. The MADs for the DFT methods range from 7 to 8 kJ mol^{-1} (for KMLYP and BMK) to approximately 30 kJ mol^{-1} (for B-LYP, B3-LYP, MPW1K and MPWPW91). Of these methods, BMK is particularly attractive because (as we saw above) it also shows excellent performance for the heats of formation (MAD 4 kJ mol^{-1}) and it does not include an empirical higher-level correction term.

An examination of Figure 2 and Table 3 reveals that all of the DFT methods suffer to a greater or lesser extent from the tendency seen previously with B3-LYP to overestimate the BDE-lowering effect accompanying increasing alkylation of R.[11] Of the various methods, B-LYP shows the largest systematic errors, predicting qualitatively incorrect behavior for the ethers and alcohols. KMLYP and BMK show the smallest systematic errors, and the other methods fall between these two extremes. However, it should be stressed that even the best DFT methods show significant systematic errors in the prediction of the relative BDEs.

As a consequence of the observed overestimation of the stabilizing effect in going from R = Me to R = *t*-Bu on the R−X BDEs, it is clear that caution needs to be exercised in applying DFT procedures to such problems. More broadly, it is likely that some of these DFT procedures would be unsuitable for studying (and hence rationalizing) the effect of substituents on bond energies, and that other important quantities that depend on relative BDEs (such as radical stabilization energies, and the enthalpies and barriers of abstraction reactions) may also be subject to considerable error. Further improvement in DFT methods (or other alternatives) capable of dealing with this problem would be desirable.

Turning our attention to the MP2-based methods, we first note that, as in the case of the DFT procedures, the absolute errors in the BDEs are much smaller than those for the heats of formation, due to a favorable cancellation of errors. The errors are also much less basis-set dependent. With the standard RMP2 method, the MADs range from approximately 15 kJ mol^{-1} (with the TZ basis set) to 20 kJ mol^{-1} (with the 6-311+G(3df,2p) and QZ basis sets). Not surprisingly then, the BDEs and their associated errors at the infinite-basis-set limit are quite similar to those with the QZ basis set. In some cases the error increases slightly, whereas in others it decreases slightly. Although the errors are smaller than for the heats of formation, the maximum errors in the standard RMP2 method are nonetheless of the order of 30 kJ mol^{-1} for the three basis sets considered, and this method is still not suitable for the accurate prediction of absolute BDEs. The SCS-MP2 and SOS-MP2 methods perform much better than standard MP2. For SCS-MP2, the MADs are 4.3 and 8.7 kJ mol^{-1} with the TZ and QZ basis sets, respectively, with corresponding maximum deviations of 11.3 and 17.2 kJ mol^{-1}. For SOS-MP2, the corresponding values are 4.3 and 4.2 kJ mol^{-1} (MADs) and 11.1 and 10.3 kJ mol^{-1} (maximum deviations). Extrapolation to an infinite basis set actually leads to worse results for all three MP2-based methods.

Although the performance of standard RMP2 is quite poor for the *absolute* BDEs, all of the MP2-based methods perform quite well for the *relative* BDEs (see Figure 2). Like G3-RAD and G3(MP2)-RAD, the RMP2 procedures slightly underestimate the stabilizing effect on the R−X BDEs of going from R = Me to R = *t*-Bu, but generally the errors in the relative BDEs are quite small and the qualitative trends are generally reasonably reproduced. Of the MP2-based methods, SOS-MP2 is particularly attractive because, as noted above, it can be framed as a fourth-order method and thus offers promise for large systems.

4. Conclusions

In the present work, we have examined the performance of a variety of lower-cost DFT and MP2-based methods for the prediction of absolute and relative R−X bond dissociation energies (BDEs) for R = Me, Et, *i*-Pr and *t*-Bu, and X = H, CH$_3$, OCH$_3$, OH and F. The results indicate that the DFT methods considered, including several "new generation" functionals (KMLYP,[16] B1B95,[17] MPW1PW91,[18] MPW1B95,[19] BB1K,[2] MPW1K,[20] MPWB1K[19] and BMK[21]), can show significant systematic errors and, in a number of cases, fail comprehensively to reproduce the correct qualitative trends in the R−X BDEs. These errors are a consequence of a systematic overestimation by all the DFT procedures of the stabilizing effect on R−X BDEs of going from R = Me to R = *t*-Bu. Of the DFT methods, KMLYP[16] and particularly BMK[21] show the smallest systematic errors in the relative BDEs, and provide reasonable performance for the absolute BDEs and heats of formation for the reactions considered. In contrast, the MP2-based methods generally show larger errors (than the best DFT methods) for the absolute heats of formation and BDEs, but better behavior for the relative BDEs. Of these procedures, SOS-MP2 is particularly promising as a method that is potentially less computationally intensive than standard MP2.

Supporting Information Available: GAUSSIAN archive entries of UB3-LYP/6-31G(d) equilibrium structures (Table S1). This material is available free of charge via the Internet at http://pubs.acs.org.

References and Notes

(1) (a) Kohn, W.; Becke, A. D.; Parr, R. G. *J. Phys. Chem.* **1996**, *100*, 12974−12980. (b) Koch, W.; Holthausen, M. C. *A Chemist*'s *Guide to Density Functional Theory*; Wiley-VCH: Weinheim, 2000.

(2) See for example: Zhao, Y.; Lynch, B. J.; Truhlar, D. G. *J. Phys. Chem. A* **2004**, *108*, 2715−2719 and references therein.

(3) Andersson, S.; Grüning, M. *J. Phys. Chem. A* **2004**, *108*, 7621−7636.

(4) Saeys, M.; Reyniers, M.-F.; Marin, G. B.; van Speybroeck, V.; Waroquier, M. *J. Phys. Chem. A* **2003**, *107*, 9147−9159.

(5) Redfern, P. C.; Zapol, P.; Curtiss, L. A.; Raghavachari, K. *J. Phys. Chem. A* **2000**, *104*, 5850−5854.

(6) Curtiss, L. A.; Raghavachari, K.; Redfern, P. C.; Pople, J. A. *J. Chem. Phys.* **2000**, *112*, 7374−7383.

(7) Brinck, T.; Lee, H.-N.; Jonsson, M. *J. Phys. Chem. A* **1999**, *103*, 7094−7104.

(8) Henry, D. J.; Parkinson, C. J.; Mayer, P. M.; Radom, L. *J. Phys. Chem. A* **2001**, *105*, 6750−6756.

(9) Coote, M. L. *J. Phys. Chem. A* **2004**, *108*, 3865−3872.

(10) Chen, C.-C.; Bozzelli, J. W. *J. Phys. Chem. A* **2003**, *107*, 4531−4546.

(11) Coote, M. L.; Pross, A.; Radom, L. In *Fundamental World of Quantum Chemistry*; Brandas, E. J., Kryachko, E. S., Eds.; Kluwer Academic Publishers. Printed in Nederlands, 2004; Vol. III, pp 563−579.

(12) Coote, M. L.; Pross, A.; Radom, L. *Org. Lett.* **2003**, *5*, 4689−4692.

(13) Zavitsas, A. A. *J. Chem. Educ.* **2001**, *78*, 417−419.

(14) Matsunaga, N.; Rogers, D. W.; Zavitsas, A. A. *J. Org. Chem.* **2003**, *68*, 3158−3172.

(15) See for example: Curtiss, L. A.; Raghavachari, K.; Redfern, P. C.; Pople, J. A. *J. Chem. Phys.* **2000**, *112*, 7374−7383.

(16) Kang, J. K.; Musgrave, C. B. *J. Chem. Phys.* **2001**, *115*, 11040−11051.

(17) Zhao, Y.; Pu, J.; Lynch, B. J.; Truhlar, D. G. *Phys. Chem. Chem. Phys.* **2004**, *6*, 673−676.

(18) Adamo, C.; Barone, V. J. *J. Chem. Phys.* **1998**, *108*, 664−675.

(19) Zhao, Y.; Truhlar, D. G. *J. Phys. Chem. A* **2004**, *108*, 6908−6918.

(20) Lynch, B. J.; Fast, P. L.; Harris, M.; Truhlar, D. G. *J. Phys. Chem. A* **2000**, *104*, 4811−4815.

(21) Boese, A. D.; Martin, J. M. L. *J. Chem. Phys.* **2004**, *121*, 3405−3416.

(22) Grimme, S. *J. Chem. Phys.* **2003**, *118*, 9095−9102.

(23) Jung, Y.; Lochan, C.; Dutoi, A. D.; Head-Gordon, M. *J. Chem. Phys.* **2004**, *121*, 9793−9802.

(24) Frisch, M. J.; Trucks, G. W.; Schlegel, H. B.; Scuseria, G. E.; Robb, M. A.; Cheeseman, J. R.; Montgomery, J. A.; T. Vreven Jr.; Kudin, K. N.; Burant, J. C.; Millam, J. M.; Iyengar, S. S.; Tomasi, J.; Barone, V.; Mennucci, B.; Cossi, M.; Scalmani, G.; Rega, N.; Petersson, G. A.; Nakatsuji, H.; Hada, M.; Ehara, M.; Toyota, K.; Fukuda, R.; Hasegawa, J.; Ishida, M.; Nakajima, T.; Honda, Y.; Kitao, O.; Nakai, H.; Klene, M.; Li, X.; Knox, J. E.; Hratchian, H. P.; Cross, J. B.; Bakken, V.; Adamo, C.; Jaramillo, J.; Gomperts, R.; Stratmann, R. E.; Yazyev, O.; Austin, A. J.; Cammi, R.; Pomelli, C.; Ochterski, J. W.; Ayala, P. Y.; Morokuma, K.; Voth, G. A.; Salvador, P.; Dannenberg, J. J.; Zakrzewski, V. G.; Dapprich, S.; Daniels, A. D.; Strain, M. C.; Farkas, O.; Malick, D. K.; Rabuck, A. D.; Raghavachari, K.; Foresman, J. B.; Ortiz, J. V.; Cui, Q.; Baboul, A. G.; Clifford, S.; Cioslowski, J.; Stefanov, B. B.; G Liu, A. L.; Piskorz, P.; Komaromi, I.; Martin, R. L.; Fox, D. J.; Keith, T.; Al-Laham, M. A.; Peng, C. Y.; Nanayakkara, A.; Challacombe, M.; Gill, P. M. W.; Johnson, B.; Chen, W.; Wong, M. W.; Gonzalez, C.; Pople, J. A. *GAUSSIAN 03,* Revision C.02; Gaussian, Inc.: Wallingford. CT, 2004.

(25) Werner, H.-J.; Knowles, P. J.; Lindh, R.; Schütz, M.; Celani, P.; Korona, T.; Manby, F. R.; Rauhut, G.; Amos, R. D.; Bernhardsson, A.; Berning, A.; Cooper, D. L.; Deegan, M. J. O.; Dobbyn, A. J.; Eckert, F.; Hampel, C.; Hetzer, G.; Lloyd, A. W.; McNicholas, S. J.; Meyer, W.; Mura, M. E.; Nicklass, A.; Palmieri, P.; Pitzer, R.; Schumann, U.; Stoll, H.; Stone, A. J.; Tarroni, R.; Thorsteinsson, T. *MOLPRO 2002.6, a package of ab initio programs*; University of Birmingham, Birmingham, U.K., 2003.

(26) Stanton, J. F.; Gauss, J.; Watts, J. D.; Nooijen, M.; Oliphant, N.; Perera, S. A.; Szalay, P. G.; Lauderdale, W. J.; Kucharski, S. A.; Gwaltney, S. R.; Beck, S.; Balková, A.; Bernholdt, D. E.; Baeck, K. K.; Rozyczko, P.; Sekino, H.; Hober, C.; Bartlett, R. J. *ACES II, Quantum Theory project*; University of Florida: Gainsville, 1992.

(27) Scott, A. P.; Radom, L. *J. Phys. Chem.* **1996**, *100*, 16502−16513.

(28) Becke, A. D. *J. Chem. Phys.* **1996**, *104*, 1040−1046.

(29) See for example: Boese, A. D.; Oren, M.; Atasoylu, O.; Martin, J. M. L.; Kállay, M.; Gauss, J. *J. Chem. Phys.* **2004**, *120*, 4129−4141.

(30) (a) Piacenza, M.; Grimme, S. *J. Comput. Chem.* **2003**, *25*, 83−98. (b) Grimme, S. *J. Phys. Chem. A* **2005**, *109*, 3067−3077.

(31) Nicolaides, A.; Rauk, A.; Glukhovtsev, M. N.; Radom, L. *J. Phys. Chem.* **1996**, *100*, 17460−17464.

(32) Linstrom, P. J., Mallard, W. G., Eds. NIST Chemistry WebBook. In *NIST Standard Reference Database No. 69*; National Institute of Standards and Technology, Gaithersburg MD, 2003; http://webbook.nist.gov.

(33) Blanksby, S. J.; Ellison, G. B. *Acc. Chem. Res.* **2003**, *36*, 255−263.

(34) Henry, D. J.; Parkinson, C. J.; Radom, L. *J. Phys. Chem. A* **2002**, *106*, 7927−7936.

(35) Gómez-Balderas, R.; Coote, M. L.; Henry, D. J.; Radom, L. *J. Phys. Chem. A* **2004**, *108*, 2874−2883.

(36) Coote, M. L.; Wood, G. P. F.; Radom, L. *J. Phys. Chem. A* **2002**, *106*, 12124−12138.

(37) See for example: Helgaker, T.; Jørgensen, P.; Olsen, J. *Molecular Electronic-Structure Theory*; John Wiley and Sons Ltd: New York, 2000.